

# Frequency-preserved non-reciprocal acoustic propagation in a granular chain

Jian-Guo Cui,<sup>1,2</sup> Tianzhi Yang,<sup>3,4,a)</sup> and Li-Qun Chen<sup>1,2,a)</sup>

<sup>1</sup>Shanghai Institute of Applied Mathematics and Mechanics, Shanghai University, Shanghai 200072, China

<sup>2</sup>Department of Mechanics, Shanghai University, Shanghai 200444, China

<sup>3</sup>Department of Mechanics, Tianjin University, Tianjin 300072, China

<sup>4</sup>Tianjin Key Laboratory of Nonlinear Dynamics and Chaos Control, Tianjin 300072, China

(Received 21 October 2017; accepted 18 April 2018; published online 2 May 2018)

Experimental evidence is presented for demonstrating frequency-preserved non-reciprocal acoustic propagation in a lower frequency range. A 23-bead granular chain and a conical rod are combined to realize this phenomenon. The conical rod is used to amplify the amplitude of the incident wave. Because of the inherent nonlinearity, this granular system offers an ideal testing platform that can provide an amplitude-dependent bandgap. By carefully tuning the taper ratio of the conical rod, a strong non-reciprocal acoustic propagation is observed. Moreover, such a phenomenon does not change the frequency of the incident wave due to the weak nonlinearity, which is different from previous studies. The result represents an advance in acoustic metamaterial systems using simple materials and paves the way for practical applications. *Published by AIP Publishing.*

<https://doi.org/10.1063/1.5009975>

The invention and development of electric diodes led to a ground-breaking revolution in technology. Rectification has been a key building block in modern electronics. Captivated by this specific characteristic, several researchers have transplanted this feature of the electric diode to other fields, such as thermodynamics and optics.<sup>1–4</sup> Compared with electrical current, vibrational and acoustic waves are ubiquitous carriers of energy in our environment. Very recently, an acoustic element-acoustic diode was invented and proved to be a smart way for acoustic energy manipulations. Some advanced acoustic elements, such as acoustic transistors<sup>5–7</sup> and logic elements,<sup>8</sup> were developed and experimentally verified. However, realizing an acoustic rectifier in a practical system has been a tough challenge, which needs to break the reciprocity. Reciprocity is a fundamental principle in wave-based systems, which requires that the response of a transmission channel is symmetric when the source and observing point are interchanged. Breaking the reciprocity has recently become a thriving research topic.<sup>9–12</sup>

Earlier attempts used nonlinear media to control the acoustic one-way propagation.<sup>5–8,13,14</sup> This strategy depends highly on the nonlinear medium<sup>15–17</sup> but provided a crucial step to achieve the goal. Among these studies, however, the frequencies of the driving signal changed and reshaped the waveform during propagation. Therefore, any acoustic information conveyed in the frequency spectrum information was changed or lost.<sup>18–24</sup> To tackle this problem, Gao *et al.* developed an acoustic diode model that can preserve the frequencies of the incident wave.<sup>25</sup> In their theoretical study, a nonlinear spring-mass system is used to generate an amplitude-dependent bandgap. However, this method had not been verified by experiments to date as there is an inherent difficulty in fabricating such cubic-nonlinearity in a nonlinear system. In this letter, we present the experimental

evidence of a frequency-preservation, low-frequency, easy-to-make acoustic diode by using a granular chain, which is not realized to date. This may inspire an alternative design of a one-way sound wall, in which the frequency information will not be changed or lost.

In this letter, we provide a simple, practically realizable example in a granular chain to achieve frequency-preserved acoustic non-reciprocal propagation, as shown in Fig. 1(a). The granular chains have been extensively studied in recent years,<sup>8,26–29</sup> as they provide an inherent platform to support nonlinear phenomena. A conical rod is attached to one end of the chain for modulating the incident wave amplitude. The force-displacement relationship between two solid spheres was proved to follow a nonlinear Hertzian contact law<sup>30</sup>

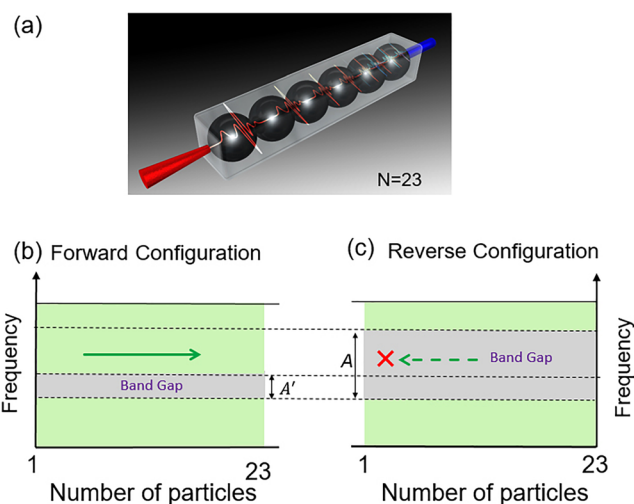


FIG. 1. Schematic and conceptual diagrams. (a) Schematic of the proposed granular device. (b) Bandgap of the granular chain;  $A$  denotes the amplitude of the input signal of the forward configuration. (c) Bandgap of the chain with a conical rod;  $A'$  denotes the amplitude of the input signal of the backward configuration. The conical rod is designed to modulate the range of forbidden bands.

<sup>a)</sup>Authors to whom corresponding should be addressed: yang@dyn.tu-darmstadt.de and lqchen@staff.shu.edu.cn

$$\frac{dF}{d\delta} = \frac{3}{2}A\delta_0^{1/2}, \quad (1)$$

where  $F$  denotes the compression force,  $\delta$  and  $\delta_0$  denote the deformation and the static pre-deformation, and  $A$  is a coefficient depending on the materials. The stiffness is seen to be a nonlinear function of  $\delta_0$ , which generates an amplitude-dependent bandgap in a chain; it is a key element in the design of the acoustic diode. In contrast, a linear periodic structure has a fixed bandgap.

The equation of motion of a vibrating chain can be expressed as a set of second-order differential equations based on the Hertz interaction law.<sup>30,31</sup> The displacement from the equilibrium position  $u_i$  is

$$\ddot{u}_i = p\eta_{i-1}^{3/2} - p\eta_i^{3/2}, \quad (2)$$

where  $\eta_i = \delta + u_{i-1} - u_i$  ( $\eta_i > 0$  else  $\eta_i = 0$ ). Here,  $i$  takes values from 2 to  $N - 1$ . In addition, considering the differences in boundary conditions, the equations for the first and last beads are expressed as

$$\ddot{u}_1 = p_{\text{act}}\eta_0^{3/2} - p\eta_1^{3/2}, \quad \ddot{u}_N = p\eta_{N-1}^{3/2} - F_0, \quad (3)$$

where  $\eta_0 = \delta_{\text{act}} + B\cos(2\pi ft) - u_1$ , with  $\eta_0 > 0$  else  $\eta_0 = 0$ . Here,  $B\cos(2\pi ft)$  denotes the excitation of the granular acoustic diode,  $B$  the driving amplitude, and  $f$  the driving frequency. In Eqs. (2) and (3),  $p = E\sqrt{2R}/[3(1-\nu^2)m]$  and  $p_{\text{act}} = \sqrt{2}p$  denote the coefficients in the Hertz interaction law. In this paper,  $E$  is the Young's modulus,  $R$  the bead radius,  $\nu$  Poisson's ratio, and  $m$  the mass of the bead.  $\delta_{\text{act}}$  and  $\delta$  are defined by Hertz's law  $\delta_{\text{act}} = [F_0/(mp)]^{2/3}$  and  $\delta = [F_0/(mp)]^{2/3}$ , with  $F_0$  the initial compression force.

Figures 1(b) and 1(c) show the mechanism of the amplitude-dependent bandgap. Here, we specify the forward direction for the case where the shaker is placed on the left side. In this direction, the amplitude and frequency of the incident wave ( $A, f$ ) is initially modulated by the conical rod and the wave amplitude is converted to  $A'$ , which may fall out of the forbidden band, thus the wave can pass through the chain. In contrast, if the same wave is excited from the backward direction with amplitude  $A$ , the converted wave may fall in of the forbidden band and be blocked.

Such an amplitude-dependent bandgap provided the inspiration to use the bandgap as an on-off switch by carefully tuning the amplitude of incident waves, inducing non-reciprocal wave propagation behavior. In our study, we use a conical rod to modulate the incident amplitude. Furthermore, the frequency of the propagating wave is not changed because of weak nonlinearity in the chain. The conical rod is a linear system, which also ensures frequency preservation. It is noted that the governing equation of the conical rod is not under consideration because, in the forward configuration, the conical rod just amplifies the input wave and thus behaves as an inputting device. In the backward configuration, the bandgap of the chain forbids wave propagation, and therefore, the rod does not vibrate.

A granular chain of finite length can support typical wave propagation behavior. We simulated our system and found that 23 beads were sufficiently accurate to realize the

dynamic feature. Narisetti *et al.*<sup>32</sup> used a perturbative approach and obtained an analytical dispersion relation for the amplitude-dependent bandgap between 1352 Hz and 1439 Hz, which is plotted in Fig. 2(a). The analytical prediction suggests that acoustic rectification may occur within this bandgap, and we used direct numerical simulation to confirm this prediction, as shown in Fig. 2(b). It is seen that they are in good agreements.

The proposed theoretical design is validated next. We fabricated a one-dimensional monoatomic granular chain using 23 beads made of polypropylene with elastic modulus  $E = 0.986$  GPa, Poisson's ratio  $\nu = 0.35$ , radius  $R = 0.016$  m, and density  $\rho = 1500$  Kg/m<sup>3</sup>. A spring with tunable spring force is used to produce the initial force. It is known that the granular system is highly tunable between strongly and weakly nonlinear regimes, depending on the initial pre-compression. In our case, we applied a spring force as 9.6 N, which ensures the weak nonlinearity condition  $B/\delta_{\text{act}} \ll 1$ . As shown in Fig. 2 and the experiment section, we controlled  $0.01 \leq B/\delta_{\text{act}} \leq 0.08$ .

For the experimental setup (Fig. 3), a conical rod having diameters  $D_1 = 0.056$  m and  $D_2 = 0.028$  m and length  $L = 0.07$  m was fabricated using a 3D printer. We used a shaker (left-hand side of the figure) to provide the input vibration. The forward/backward configuration is shown in Figs. 3(a) and 3(b). Moreover, we restrict the motion in the other directions. In experiments, two accelerometers were placed on the ends of the chain to measure the input and output signals. We also placed a force sensor to monitor and control the level of excitation. In addition, we also performed experiments without the conical rod for reference.

Both the input and output signals were recorded using a dynamic signal analyzer (LMS SCADAS), which also provides the input signal to the shaker. The shaker applies a constant low-amplitude displacement  $A_{\text{in}} = 4 \times 10^{-8}$  m while sweeping the frequency from 300 Hz to 2000 Hz. The normalized transmission spectra of the spherical granular chains with and without the conical rod are presented in Fig. 4. Note that the normalized transmission spectrum is defined as  $\|A_{\text{out}}/A_{\text{in}}\|$ , where  $A_{\text{in}}$  and  $A_{\text{out}}$  are the input and output amplitudes. It expresses the criteria for the transmission of acoustic signals in structure, as the acoustic signal passes through the system substantially without loss when the transmission rate approaches

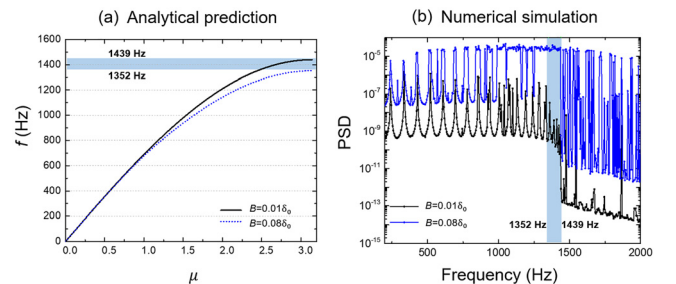


FIG. 2. Theoretical prediction of the dispersion of the granular chain. (a) Analytical prediction of the bandgap based on Ref. 32. The solid black and dotted blue lines represent the incident wave amplitudes  $B = 0.01\delta_0$  and  $0.08\delta_0$ , respectively.  $\delta_0 = 2 \times 10^{-5}$  m denotes the value of the initial deformation.  $\mu$  is the dimensionless wavenumber, ranging from 0 to  $\pi$ . (b) Numerical confirmation of the bandgap. The blue and black lines represent the incident wave amplitudes  $B = 0.01\delta_0$  and  $0.08\delta_0$ , respectively.

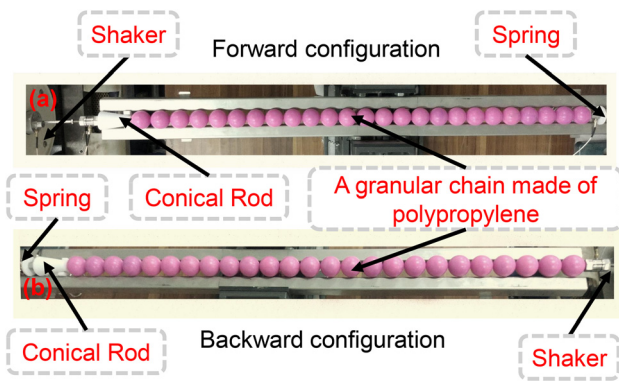


FIG. 3. Photograph of the experimental setup. (a) Experimental setup of the forward configuration with a conical rod. (b) Experimental setup of the backward configuration with a conical rod. A force sensor and two acceleration sensors are used to measure experimental data.

1. Figure 4(a) shows the measured transmission; the black and blue lines denote the forward and backward transmittances, respectively. It is seen that the backward transmittance curve has a drop between 1300 Hz and 1500 Hz, showing a clear attenuation in the forbidden bandgap. Moreover, the forward transmission is found to be more prominent than backward transmission (about 10 times), indicating an obvious non-reciprocal phenomenon for the system with the conical rod. For comparison, Fig. 4(b) shows the transmission spectrum of the reference chain without the conical rod. It is seen that the forward transmission and backward transmission are nearly identical, and no attenuation occurs in the measured frequency range. We further examine this phenomenon in the time domain. The shaker is controlled to excite at a constant frequency  $f = 1400$  Hz. As shown in Fig. 4(c), the magnitude of the forward response is much larger than the backward

response (at 1400 Hz), confirming the evident frequency-preserved non-reciprocal phenomenon.

In contrast, reciprocal propagation is observed in the reference chain [see Fig. 4(d)]. The above measured data roughly agree with theoretical prediction (Fig. 2). This rectification frequency range is much lower than that in Ref. 8, indicating a promising application in low-frequency vibration isolation, noise control, and enhanced sound sensing.

To quantify the asymmetric transmission, here we use the contrast ratio to characterize the system, defined as  $R_c = \frac{T_L - T_R}{T_L + T_R}$ ,<sup>33</sup> where subscripts  $L$  and  $R$  signify the transmission of the input signal transmitting from left-to-right and its reverse, respectively. From Fig. 5(a), the rectification ratio is calculated over the bandgap. The averaging contrast ratio is about 0.9 within the bandgap, confirming that the acoustic transmission is non-reciprocal (for reciprocal propagation,  $R_c \approx 0$ ). Finally, to further confirm our experimental evidence, we calculated the energy level of the last bead as a function of the driving amplitude. Three different frequencies were chosen in the simulation using the Runge–Kutta method. From Fig. 5(b), an abrupt energy jump takes place at 1400 Hz, corresponding to the predicted bandgap. In contrast, no jump is observed outside the bandgap, and thus, the results of the simulation align with those of experiment.

It is noted that our work is distinctly different from Ref. 8. First, the frequency of the propagating wave is preserved in this work; in contrast, the frequency is changed in Ref. 8. Second, we have realized a low-frequency ( $\sim 1400$  Hz) non-reciprocal system, which is much lower than the working frequency ( $\sim 10.5$  KHz) in Ref. 8. Third, in Ref. 8, a defect chain was used, whereas we used 23 identical beads. Finally, our work and that in Ref. 8 are based on different principles. Ref. 8 presents an acoustic rectification at a bifurcation point.

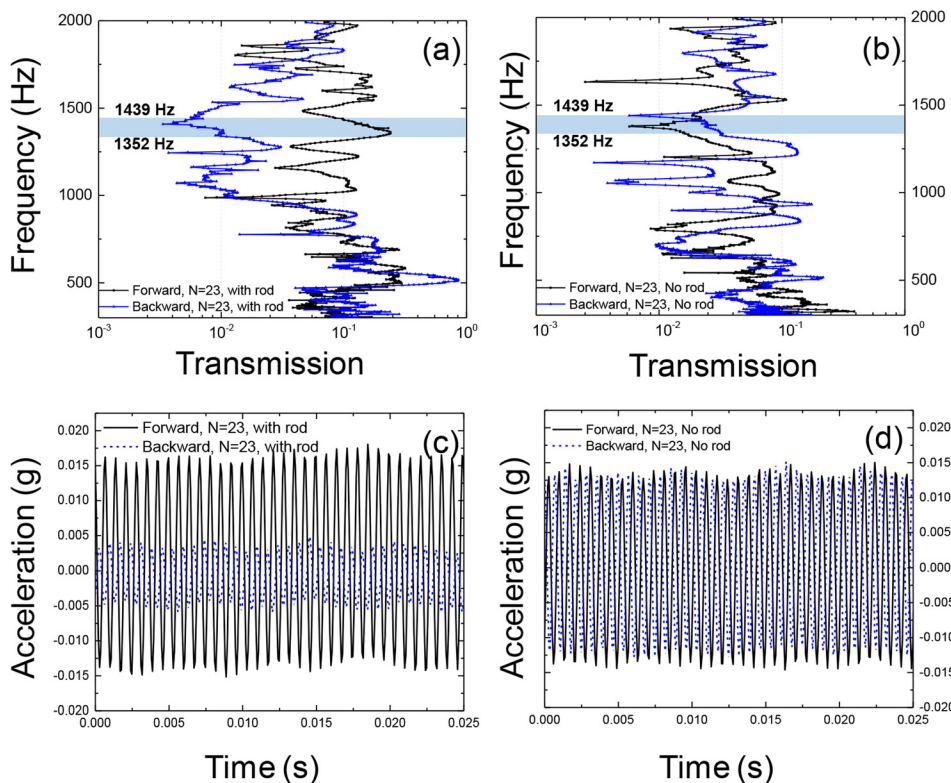


FIG. 4. The measured transmission spectra of the granular chain. (a) Transmission spectra with a conical rod. (b) Transmission spectra without the conical rod. In (a) and (b), the solid black line denotes the forward transmission and the solid blue line denotes the backward transmission, respectively. (c) Time history of the non-reciprocal phenomenon (with rod). (d) Time history of the reciprocal phenomenon (without rod).

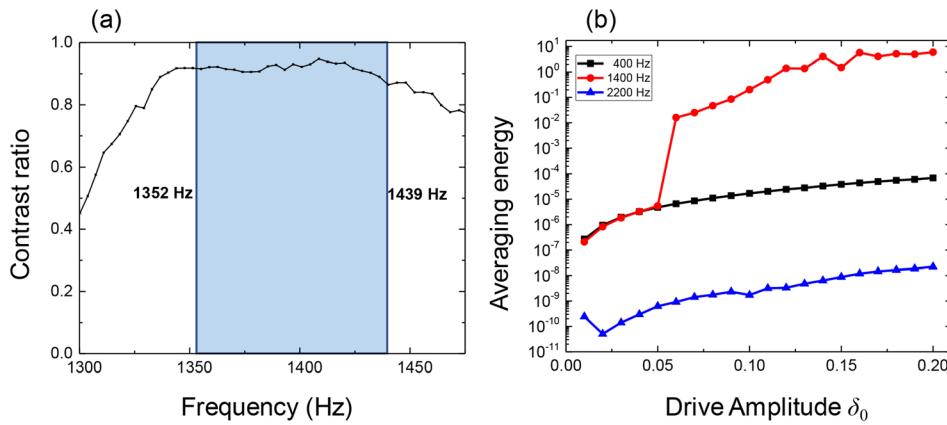


FIG. 5. Contrast ratio and energy level. (a) The contrast ratio associated with non-reciprocal propagation. (b) Energy level of the last bead as a function of the driving amplitude. The solid black, red, and blue lines denote the response of the last bead at 400 Hz (outside the bandgap), 1400 Hz (within the bandgap), and 2200 Hz (outside the bandgap), respectively.

In contrast, we realized non-reciprocal behavior through carefully tuning the incident wave amplitude.

In conclusion, we have presented experimental evidence of non-reciprocal acoustic propagation in a simple 1D granular chain. The inherent nonlinearity of the chain exhibits amplitude-dependent bandgaps. A conical rod is used to change the input amplitude, thereby switching the bandgap on and off. We have shown that it is possible to break reciprocity in a simple granular system, realizing vastly different output response under excitation from different sides. Due to the weakly nonlinearity, the granular system can rectify the incident wave without converting its frequency. Moreover, such a system does not require a precise design and fabrication, which may lead to an alternative acoustic metamaterial design in a simple style. It is noted that the operating frequency regime falls within the audible range (around 1400 Hz), and this may inspire an alternative design of a one-way sound wall, which will not lose or change the information of the sound carries.

We are grateful to the National Science Foundation of China (Nos. 11672187 and 11572182), the Natural Science Foundation of Liaoning Province (201602573), and the Innovation Program of Shanghai Municipal Education Commission (No. 2017-01-07-00-09-E00019).

<sup>1</sup>B. Li, J. Lan, and L. Wang, *Phys. Rev. Lett.* **95**, 104302 (2005).

<sup>2</sup>C. W. Chang, D. Okawa, A. Majumdar, and A. Zettl, *Science* **314**, 1121 (2006).

<sup>3</sup>W. Kobayashi, Y. Teraoka, and I. Terasaki, *Appl. Phys. Lett.* **95**, 171905 (2009).

<sup>4</sup>X. Huang, Y. Lai, Z. H. Hang, H. Zheng, and C. T. Chan, *Nat. Mater.* **10**, 582 (2011).

<sup>5</sup>B. Liang, X. S. Guo, J. Tu, D. Zhang, and J. C. Cheng, *Nat. Mater.* **9**, 989 (2010).

<sup>6</sup>J. H. Oh, H. W. Kim, P. S. Ma, H. M. Seung, and Y. Y. Kim, *Appl. Phys. Lett.* **100**, 213503 (2012).

<sup>7</sup>A. Cicek, O. A. Kaya, and B. Ulug, *Appl. Phys. Lett.* **100**, 111905 (2012).

<sup>8</sup>N. Boechler, G. Theocharis, and C. Daraio, *Nat. Mater.* **10**, 665 (2011).

<sup>9</sup>S. Y. Lin, E. Chow, V. Hietala, P. R. Villeneuve, and J. D. Joannopoulos, *Science* **282**, 274 (1998).

<sup>10</sup>C. Daraio, V. F. Nesterenko, E. B. Herbold, and S. Jin, *Phys. Rev. E* **73**, 026610 (2006).

<sup>11</sup>B. P. Bernard, M. J. Mazzoleni, N. Garraud, D. P. Arnold, and B. P. Mann, *J. Appl. Phys.* **116**, 084904 (2014).

<sup>12</sup>M. A. Hasan, S. Cho, K. Remick, A. F. Vakakis, D. M. McFarland, and W. M. Kriven, *Granular Matter* **17**, 49 (2015).

<sup>13</sup>R. Fleury, D. L. Sounas, C. F. Sieck, M. R. Haberman, and A. Alù, *Science* **343**, 516 (2014).

<sup>14</sup>X. Zhu, X. Zou, B. Liang, and J. Cheng, *J. Appl. Phys.* **108**, 124909 (2010).

<sup>15</sup>L. L. Chang, L. Esaki, and R. Tsu, *Appl. Phys. Lett.* **24**, 593 (1974).

<sup>16</sup>S. Benchabane, A. Khelif, J. Y. Rauch, L. Robert, and V. Laude, *Phys. Rev. E* **73**, 065601 (2006).

<sup>17</sup>J. O. Vasseur, A. C. Hladky-Hennion, B. Djafari-Rouhani, F. Duval, B. Dubus, Y. Pennec, and P. A. Deymier, *J. Appl. Phys.* **101**, 114904 (2007).

<sup>18</sup>V. F. Nesterenko, C. Daraio, E. B. Herbold, and S. Jin, *Phys. Rev. Lett.* **95**, 158702 (2005).

<sup>19</sup>V. F. Nesterenko, *Dynamics of Heterogeneous Materials* (Springer, New York, 2001).

<sup>20</sup>C. Coste, E. Falcon, and S. Fauve, *Phys. Rev. E* **56**, 6104 (1997).

<sup>21</sup>E. B. Herbold, J. Kim, V. F. Nesterenko, S. Y. Wang, and C. Daraio, *Acta Mech.* **205**, 85 (2009).

<sup>22</sup>A. C. Hladky-Hennion and M. D. Billy, *J. Acoust. Soc. Am.* **122**, 2594 (2007).

<sup>23</sup>N. Boechler, G. Theocharis, S. Job, P. G. Kevrekidis, M. A. Porter, and C. Daraio, *Phys. Rev. Lett.* **104**, 244302 (2010).

<sup>24</sup>S. Job, F. Santibanez, F. Tapia, and F. Melo, *Phys. Rev. E* **80**, 025602 (2009).

<sup>25</sup>C. Liu, Z. Du, Z. Sun, H. Gao, and X. Guo, *Phys. Rev. Appl.* **3**, 064014 (2015).

<sup>26</sup>N. Boechler, J. Yang, G. Theocharis, P. G. Kevrekidis, and C. Daraio, *J. Appl. Phys.* **109**, 074906 (2011).

<sup>27</sup>Y. Man, N. Boechler, G. Theocharis, P. G. Kevrekidis, and C. Daraio, *Phys. Rev. E* **85**, 037601 (2012).

<sup>28</sup>H. A. Burgoyne and C. Daraio, *J. Appl. Mech.* **82**, 081002 (2015).

<sup>29</sup>J. Lydon, G. Theogrios, and C. Daraio, *Phys. Rev. E* **91**, 023208 (2015).

<sup>30</sup>B. J. Briscoe, *Tribol. Int.* **19**, 109 (1986).

<sup>31</sup>H. Hertz, *J. Reine Angew. Math.* **92**, 156–171 (1882).

<sup>32</sup>R. K. Narisetti, Ph.D. thesis, Georgia Institute of Technology, 2010.

<sup>33</sup>H. Sun, S. Zhang, and X. Shui, *Appl. Phys. Lett.* **100**, 103507 (2012).